

Curing and Mechanical Properties of Dicyanate/Poly(ether sulfone) Semi-Interpenetrating Polymer Networks

Seung-Sang Roh, Bong-Taek Hong, Dae Su Kim

Department of Chemical Engineering, Chungbuk National University, San 48, Kaesin-dong, Cheongju, 361-763 Korea

Received 13 July 2001; accepted 22 April 2002

ABSTRACT: Semi-interpenetrating polymer networks (semi-IPNs) composed of a dicyanate resin and a poly(ether sulfone) (PES) were prepared, and their curing behavior and mechanical properties were investigated. The curing behavior of the dicyanate/PES semi-IPN systems catalyzed by an organic metal salt was analyzed. Differential scanning calorimetry was used to study the curing behavior of the semi-IPN systems. The curing rate of the semi-IPN systems decreased as the PES content increased. An autocatalytic reaction mechanism was used to analyze the curing reaction of

the semi-IPN systems. The glass-transition temperature of the semi-IPNs decreased with increasing PES content. The thermal decomposition behavior of the semi-IPNs was investigated. The morphology of the semi-IPNs was investigated with scanning electron microscopy. © 2002 Wiley Periodicals, Inc. *J Appl Polym Sci* 87: 1079–1084, 2003

Key words: kinetics (polym.); poly(ether sulfone); interpenetrating polymer networks (IPN)

INTRODUCTION

Dicyanate resins are low-viscosity resins that can crosslink to form polycyanurates by forming very thermally stable cyclic triazine rings. Polycyanurates possess high glass-transition temperatures ($T_g = 250$ – 290°C), low water absorption, low dielectric properties, and excellent processability and compatibility with reinforced fibers.¹ The dicyanate resins combine the processing advantages and handling convenience of epoxy resins, the fire resistance of phenolic resins, and the high-temperature performance of polysulfones or polyimides. Recent studies have focused on their potential matrix applications in advanced composites and electronics.^{2–6}

In general, for the toughening of highly crosslinked thermosets, rubbers have been used as impact modifiers. However, there has been little success because the yielding of thermosetting matrices cannot be induced on account of the highly crosslinked structures. Therefore, the toughening of highly crosslinked thermosets was achieved by physical blending with high-performance engineering thermoplastics such as poly(ether imide)s and polysulfones. This concept of semi-interpenetrating polymer networks (semi-IPNs) has been successfully applied to the development of tough and thermally stable matrix resins for advanced fiber-reinforced polymer composites.^{7–11} Such semi-IPNs can be processed like thermosets and show notable

improvements in the fracture toughness and microcracking resistance of fiber-reinforced composites over unmodified thermosetting composites.¹² The toughening mechanism generally depends on the morphology of the semi-IPNs developed by the phase-separation process occurring during curing.

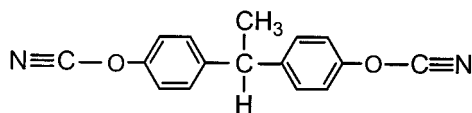
In this study, a poly(ether sulfone) (PES) was employed as a thermoplastic to make semi-IPNs with a dicyanate resin. Generally, PESs are clear, rigid, and tough thermoplastics with T_g 's of 180 – 250°C . Understanding the curing kinetics of a semi-IPN system is important in optimizing polymer processing conditions and in producing polymer products constituting the semi-IPN with excellent quality. Therefore, dicyanate/PES semi-IPN systems with different compositions were formulated, and their curing behavior and some physical properties were investigated as functions of the composition and curing condition.

EXPERIMENTAL

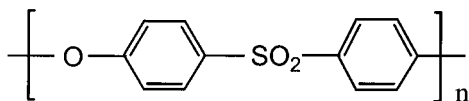
Materials

The dicyanate resin used in this study was 1,1-bis(4-cyanatophenyl) ethane (Arocy L-10 from Ciba Specialty Chemicals, Summit, NJ). The amorphous thermoplastic polymer used to modify the dicyanate resin was PES (Ultrason E6020P from BASF, Mount Olive, NJ). The resins were used as received. Figure 1 shows the chemical structures of the resins. The organic metal salt used to catalyze the cyanate polymerization was zinc stearate. The catalyst content in all the semi-IPN formulations was fixed to 0.1 phr (parts per hundred of dicyanate resin) according to the previous

Correspondence to: D. S. Kim (dskim@chungbuk.ac.kr).



1,1-bis(4-cyanatophenyl) ethane (Arocy L-10)



Polyethersulfone (Ultrason E6020P)

Figure 1 Chemical structures of the dicyanate and PES resin.

results.¹³ Methylene chloride (CH_2Cl_2) was used as a cosolvent for both resins to make homogeneous resin solutions. The resin content in each solution was 30 wt %.

Measurements

Differential scanning calorimetry (DSC)

To investigate the curing behavior of the dicyanate/PES semi-IPN systems, we used a DSC 2910 (TA Instruments, New Castle, DE). The DSC sample preparation procedure was as follows. First, zinc stearate was dissolved in the dicyanate resin, and the PES resin was dissolved in methylene chloride. A homogeneous solution was prepared by the mixing of the two mixtures at room temperature. A homogeneous dicyanate/PES semi-IPN system was prepared by the removal of the solvent from the solution in a vacuum oven. About 10 mg of the semi-IPN system was placed in a hermetic aluminum sample pan and tested immediately after sealing. The amount of PES in the semi-IPN systems was varied from 0 to 30 phr. Each sample was cured dynamically at different heating rates of 5, 10, or 20°C/min. The dynamic DSC scans were carried out from room temperature to 350°C under a nitrogen gas atmosphere. Second DSC scans were carried out at a heating rate of 10°C/min so that the glass transition of each semi-IPN could be monitored.

Dynamic mechanical analysis (DMA)

DMA was carried out with a DMA 2940 (TA Instruments) in a single-cantilever mode to measure the mechanical properties of the dicyanate/PES semi-IPNs. Each sample specimen was prepared by the degassed dicyanate/PES system being poured into a mold and then cured. The mold was composed of a silicon rubber spacer (35 mm × 13 mm × 3.2 mm) and two steel plates. The curing condition was 150°C for

2 h and 180°C for 1 h. Each sample specimen was postcured at 200°C for 0.5 h. DMA was performed from room temperature to 300°C at 5°C/min. The frequency was 1 Hz.

Thermogravimetric analysis

To investigate the thermal decomposition behavior of the dicyanate/PES semi-IPNs, an SDT 2960 (TA Instruments) was used. Each scan was performed from room temperature to 800°C at a heating rate of 10°C/min under a nitrogen gas atmosphere. The samples were taken from the semi-IPN sheets prepared for DMA.

Scanning electron microscopy (SEM)

The morphology of the fracture surfaces of the semi-IPNs was investigated with a Hitachi S-2500C scanning electron microscope (Tokyo, Japan). Each sample was coated with a gold sputterer.

RESULTS AND DISCUSSION

Curing kinetics

Figure 2 shows dynamic DSC thermograms of the dicyanate/PES semi-IPN systems with various PES contents. The DSC thermograms were measured at a heating rate of 10°C/min. The curing rate of the semi-IPN system decreased as the PES content was increased.

The curing behavior of cyanate resins has been studied by several researchers.^{14–17} It has been found that the reaction kinetics of cyanate trimerization can be described by simple n th-order Arrhenius-type equa-

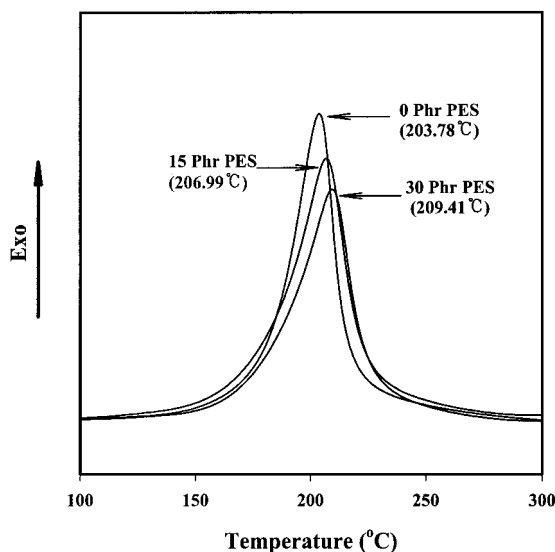


Figure 2 Dynamic DSC thermograms of the dicyanate/PES systems with various PES contents.

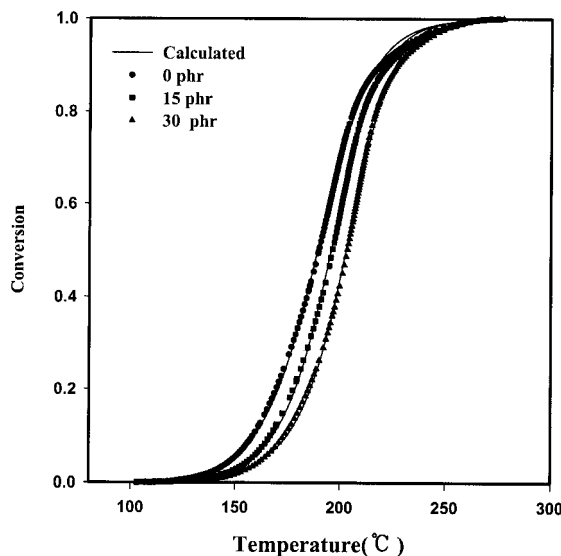


Figure 3 Comparison of the conversions measured from DSC (points) and calculated from the kinetic equation (curves) for the dicyanate/PES systems with various PES contents.

tions in the kinetic-controlled regime for catalyzed cyanate systems. The following autocatalytic kinetic equation has been used to analyze the reaction kinetics of cyanate resin systems:

$$\frac{d\alpha}{dt} = (k_1 + k_2\alpha^p)(1 - \alpha)^{n-p} \quad (1)$$

where α is the conversion, p is the reaction order associated with the autocatalytic reaction, and n is the overall reaction order. The reaction rate constants, k_1 and k_2 , follow an Arrhenius dependence on temperature and can be described as follows:

$$k_1 = k_{11} \exp\left(-\frac{E_1}{RT}\right) \quad (2)$$

$$k_2 = k_{22} \exp\left(-\frac{E_2}{RT}\right) \quad (3)$$

where k_{11} and k_{22} are frequency factors, E_1 and E_2 are activation energies, and R is the ideal gas constant.

The autocatalytic reaction kinetic equation can be expressed as follows, by the introduction of eqs. (2) and (3), if we assume that n is 2:

$$\frac{d\alpha}{dT} = \frac{1}{S_r} \left[k_{11} \exp\left(-\frac{E_1}{RT}\right) + k_{22} \exp\left(-\frac{E_2}{RT}\right) \alpha^p \right] (1 - \alpha)^{2-p} \quad (4)$$

where S_r is the scanning rate used in the dynamic DSC experiments.

The dynamic DSC method was used to obtain the parameters of the reaction kinetic equation for the semi-IPN systems. The exothermic reaction heats produced during the curing reaction of the semi-IPN systems were measured by DSC. The chemical conversion was assumed to be the ratio of the heat generated until a certain temperature to the overall heat of reaction at complete conversion ($\alpha = 1$). The conversion data obtained from the dynamic DSC exotherms (Fig. 2) of the semi-IPN systems are shown as symbols in Figure 3. The parameters of the reaction kinetic equations were determined by the fitting of the kinetic equation to the dynamic DSC conversion data shown in Figure 3.¹⁸ The fitting results are shown in Figure 3 as curves. The conversion data obtained from the dynamic DSC exotherms agree fairly well with the fitting curves calculated from the reaction kinetic equation for the semi-IPN systems. The slight deviations of the kinetic model at high conversion ranges seem to be due to a diffusion-controlled curing reaction mechanism of the semi-IPN systems after gelation. The reaction kinetic parameters (k_{11} , k_{22} , E_1 , E_2 , and p) for the dicyanate/PES semi-IPN systems with various PES contents are listed in Table I.

Figure 4 shows the DSC thermograms of the semi-IPN systems containing 15 phr PES for various heating rates. The peak temperature of the thermogram shifted to a higher temperature region as the heating rate was increased. The peak temperature shift due to the increasing heating rate depended on the activation energy associated with each reaction. On the basis of this peak-shifting phenomenon, two simple methods, by Kissinger¹⁹ and by Ozawa²⁰ and Flynn,²¹ were used to calculate the activation energy associated with each reaction. However, the nonlinear regression method was used in this work to analyze the reaction kinetics of the semi-IPN systems more precisely. Figure 5 shows that the conversion data obtained from the dynamic DSC exotherms agreed well with the conversion curves calculated from the reaction kinetic equation for the semi-IPN system containing 15 phr PES.

TABLE I
Values of Reaction Kinetic Parameters for the Dicyanate/PES Semi-IPN Systems

PES content (phr)	k_{11} (1/s)	k_{22} (1/s)	E_1 (J/mol)	E_2 (J/mol)	p
0	3.15×10^7	1.42×10^{11}	1.78×10^4	2.41×10^4	0.37
15	4.76×10^5	1.42×10^{11}	1.47×10^4	2.42×10^4	0.42
30	2.80×10^6	1.42×10^{11}	1.64×10^4	2.46×10^4	0.53

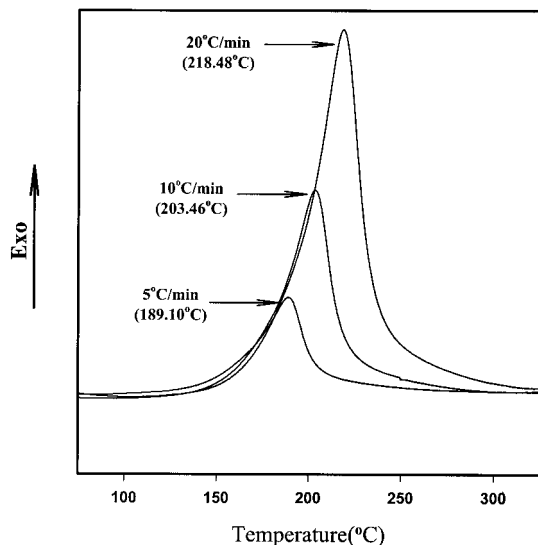


Figure 4 Dynamic DSC thermograms of the dicyanate/PES system containing 15 phr PES.

T_g 's of the dicyanate/PES semi-IPNs were measured by DSC at a heating rate of 10°C/min. Figure 6 shows that T_g of the semi-IPN decreased as the PES content was increased. The result was reasonable because T_g of PES was lower than T_g of the dicyanate resin. A distinct phase separation of the semi-IPN system was not observed in the DSC thermograms up to a PES content of 15 phr. However, for the semi-IPN containing 30 phr PES, two glass transitions indicating two phases developed by the phase-separation process during curing were observed. It is thought that

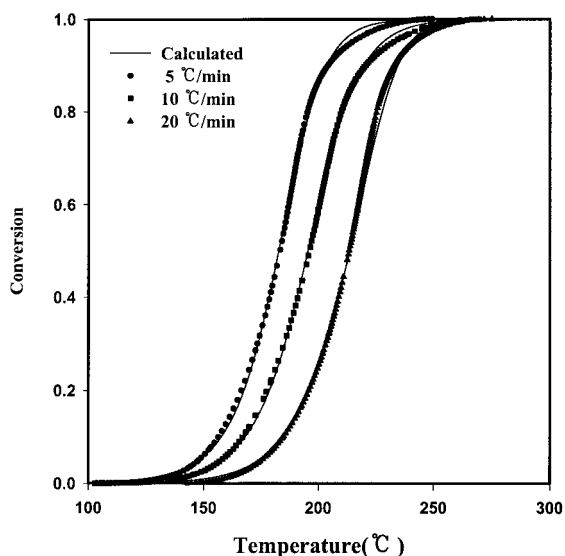


Figure 5 Comparison of the conversions measured from DSC (points) and calculated from the kinetic equation (curves) for the dicyanate/PES system containing 15 phr PES.

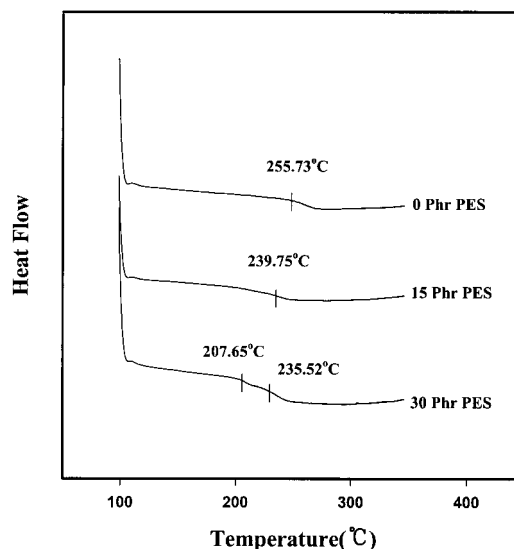


Figure 6 Glass transitions of the dicyanate/PES systems with various PES contents.

the lower T_g was for the PES-rich phase and the higher T_g was for the dicyanate-rich phase.

Dynamic mechanical properties

Figure 7 shows the storage and loss moduli of the semi-IPN systems with various PES contents measured at a heating rate of 5°C/min. The modulus of the semi-IPNs containing PES was a little bit lower than that of the pure dicyanate resin in the glassy region. T_g of the semi-IPN, determined from the sharply decreasing region in the storage modulus curve, decreased as the PES content was increased. In a comparison of the T_g results obtained from the DSC

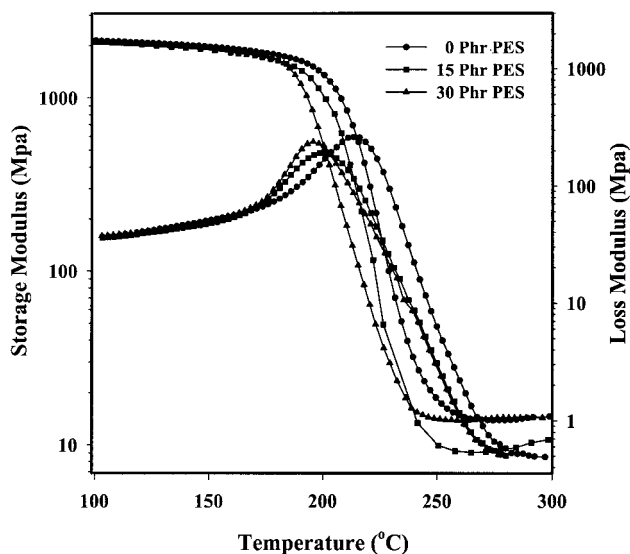


Figure 7 Storage and loss moduli of the semi-IPNs with various PES contents.

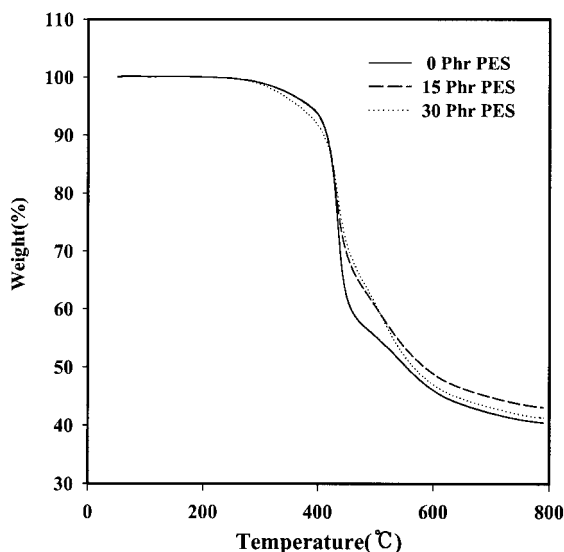


Figure 8 Weight losses of the dicyanate/PES systems during heating.

scans, the two distinct glass transitions were not observed from the DMA curves even for the semi-IPN with 30 phr PES. This result might have been caused by the relatively lower heating rate in DMA, which was used for the thermal equilibrium between the samples and the DMA instrument.

Thermal stability

Figure 8 shows the thermal degradation behavior of the dicyanate/PES semi-IPNs with various PES contents measured at a heating rate of 10°C/min. The onset temperature of the thermal degradation process shifted slightly to a lower temperature region with increasing PES content. This result seems to have been caused by the reduced crosslinking density of the polycyanurate network due to the introduction of PES.

Morphology

SEM micrographs of the dicyanate/PES semi-IPNs with various PES contents are shown in Figure 9. The fracture surface of each semi-IPN sample was investigated so that the morphology of the semi-IPNs could be analyzed. In contrast to the single-phase morphology of the pure dicyanate resin and the semi-IPN containing 15 phr PES, the fracture surface of the semi-IPN containing 30 phr PES showed a discrete-continuous morphology, with the matrix phase continuously interconnected and with the other appearing as discrete spherical particles (ca. 1 μ m in diameter) hidden inside the continuous matrix phase. The fracture surface of the pure dicyanate resin showed brittle failure behavior. However, the fracture surfaces of the semi-IPNs showed ductile failure behavior indicating the improved toughness of the semi-IPNs.

CONCLUSIONS

The effects of altering the PES content and curing conditions on the curing behavior, thermomechanical properties, and morphology of dicyanate/PES semi-IPN systems were analyzed. The curing rate of the semi-IPN systems decreased as the PES content was increased. The reaction kinetics of the semi-IPN systems could be described fairly well by a second-order autocatalytic kinetic equation. The reaction kinetic parameters were determined from the dynamic DSC conversion data by a fitting method. T_g 's of the dicyanate/PES semi-IPNs decreased with increasing PES content. For the semi-IPN containing 30 phr PES, two glass transitions indicating phase separation were observed. The thermal decomposition process of the semi-IPNs was retarded slightly with decreasing PES content. SEM micrographs showed a phase-separated morphology and different fracture characteristics for the dicyanate/PES semi-IPN systems.

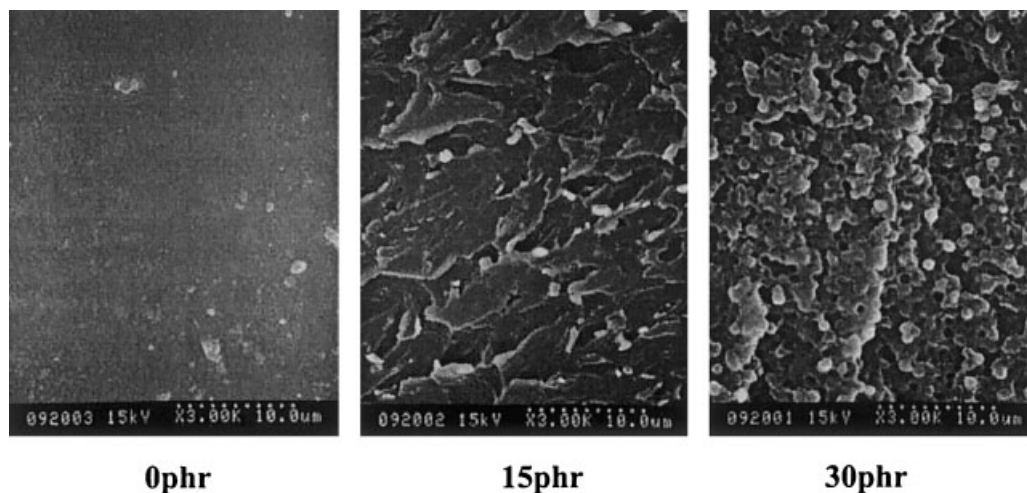


Figure 9 SEM micrographs of the dicyanate/PES systems with various PES contents.

References

1. Shimp, D. A. SAMPE Q 1987, 19, 41.
2. Papathomas, K. L.; Wang, D. W. J Appl Polym Sci 1992, 44, 1267.
3. Osei-Owusu, A.; Martin, G. C.; Gotro, J. T. Polym Eng Sci 1991, 31, 1604.
4. Zeng, S.; Ahn, K. J.; Sereris, J. C.; Kenny, J. M.; Nicolais, L. Polym Compos 1992, 13, 191.
5. Simon, S. L.; Gillham, J. K. J Appl Polym Sci 1993, 47, 461.
6. Mehrkam, P.; Cochran, R. Proc Tech Conf Am Soc Compos 1992, 7, 12.
7. Pater, R. H. Polym Eng Sci 1991, 31, 20.
8. Zeng, H.; Mai, K. Macromol Chem 1986, 187, 1787.
9. Yamamoto, Y.; Datoh, S.; Etoh, S. SAMPE J 1986, 21, 6.
10. Pascal, T.; Mercier, R.; Sillion, B. Polymer 1989, 30, 739.
11. Jang, B. Z.; Pater, R. H.; Soucek, M. D.; Hinkley, J. A. J Polym Sci Part B: Polym Phys 1992, 30, 643.
12. Kanky, A. O.; St. Clair, T. L. SAMPE J 1985, 21, 40.
13. Kim, D. S.; Hong, B. T. Polymer (Korea) 1997, 21, 252.
14. Osei-Owusu, A.; Martin, G. C.; Groto, J. T. Polym Eng Sci 1991, 32, 1604.
15. Gupta, A.; Macosko, C. W. Macromolecules 1993, 26, 2455.
16. Simon, S. L.; Gillham, J. K.; Shimp, D. A. Proc Am Chem Soc Div Polym Mater Sci Eng 1990, 62, 96.
17. Kamal, M. R.; Sourour, S. Polym Eng Sci 1973, 13, 59.
18. Kuester, J. L.; Mize, J. M. Optimization Techniques with FORTRAN; McGraw-Hill: New York, 1973.
19. Kissinger, H. E. Anal Chem 1957, 29, 1706.
20. Ozawa, T. J. J Therm Anal 1976, 9, 217.
21. Flynn, J. H. Therm Acta 1980, 37, 225.